Chemical Physics 91 (1984) 293–304
North-Holland, Amsterdam

VIBRATIONAL-STATE-SELECTED ION–MOLECULE REACTION CROSS SECTIONS AT THERMAL ENERGIES

D. VAN PIJKEREN, E. BOLTJES, J. VAN ECK and A. NIEHAUS

Fysisch Laboratorium, Rijksuniversiteit Utrecht, Princetonplein 5, 3584 CC Utrecht, The Netherlands

Received 25 June 1984

A method designed to measure relative ion–molecule reaction rates at thermal collision energies for selected reactant ion vibrational states is described. Relative reaction rates are determined for the three endothermic reactions: $H_2^+(v)$(He, H)HeH^+, $H_2^+(v)$(Ne, H)NeH^+, $D_2^+(v)$(Ne, D)NeD^+, and for the two exothermic reactions $H_2^+(v)$(H_2, H)H_3^+, $D_2^+(v)$(D_2, D)D_3^+, whereby data are evaluated for $v = 0$–8 for H_2^+ and for $v = 0$–12 in the case of D_2^+. The results are analyzed in terms of a modified statistical model designed for reactions that go through a collision complex. It is found that all data can be satisfactorily described within this model.

1. Introduction

We present experimental data on the following ion–molecule reactions at thermal collision energy:

$$H_2^+(v) + He \rightarrow HeH^+ + H, \quad (1)$$

$$H_2^+(v) + Ne \rightarrow NeH^+ + H, \quad (2a)$$

$$D_2^+(v) + Ne \rightarrow NeD^+ + D, \quad (2b)$$

$$H_2^+(v) + H_2 \rightarrow H_3^+ + H, \quad (3a)$$

$$D_2^+(v) + D_2 \rightarrow D_3^+ + D. \quad (3b)$$

Reactions (1) and (2) are endothermic, and reaction (3) is exothermic. The relative reaction rates are determined as a function of vibrational state (v) of $H_2^+(v)$ and $D_2^+(v)$, for values $v = 0$–8 and $v = 0$–12 respectively. The experimental method applied is a photoelectron–product ion delayed coincidence method, in which the vibrational state of the reactant ion is labelled by measuring the energy-analyzed photoelectron, emitted in the photoionization process that has created the reactant ion, in coincidence with the product ion that has been formed in a collision with the reactant ion. Preliminary data on reactions (1), (2a) and (3a) have already been reported, together with a short description of the method [1]. Here we present the additional data on reactions (2b) and (3b), give a more comprehensive description of the method, and include a discussion of the whole set of data in terms of a modified statistical model for ion–molecule reactions that go through a complex [2].

Experimental data on vibrational-state-selected reaction rates for H_2^+ have been published earlier by Chupka et al. [3,4], who used threshold photoionization mass spectrometry; by Koyano and Tanaka [5], and Tanaka et al. [6], who applied a threshold electron-secondary ion-coincidence method called TESICO; and by Anderson et al. [7,8] who combined threshold photoionization with a radio-frequency guided beam technique. In all this earlier work, data are evaluated only for $v = 0$ to 4, so that our data extend this earlier work.

In addition, our data complement the earlier data obtained by the two last mentioned methods in that they are obtained for strictly thermal energies. A detailed comparison with earlier work will be given in connection with the presentation of our results.

2. Experimental arrangement

Our apparatus consists mainly of three parts (see fig. 1): an electron spectrometer, a gas dis-

0301-0104/84/$03.00

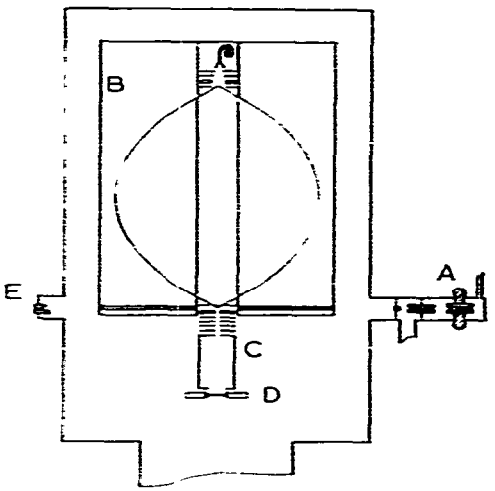

Fig. 1. Schematic view of the apparatus. A: light source; B: electron spectrometer; C: acceleration electrodes and drift region; D: channel plate; E: photon beam detector

charge lamp and a time-of-flight mass spectrometer. The different parts will be discribed shortly hereafter.

The electron spectrometer is a cylindrical mirror analyser [9–11] and consists of two concentric cylinders of 47.2 and 251.5 mm diameter. The source volume, defined by a ring slit, is 1 mm^3. The distance between source and image points is 287.3 mm.

In designing the spectrometer we tried to optimize the solid angle of acceptance for a given energy resolution. This led us to the choice of an angular range of acceptance centered around an angle of 60° with respect to the symmetry axis. In combination with slits of 2 mm width in the inner cylinder this results in a solid angle of acceptance of 2% of 4π. The energy resolution is 1%. The electrons that re-enter the volume within the inner cylinder and pass an electrode with an annular slit are accelerated to 200 eV and detected by a channeltron.

Because of the long pathlength and the low velocities of the electrons in the spectrometer the magnetic field must be smaller than 0.5×10^{-7} T. For this reason the entire spectrometer is made of aluminium and placed inside a double μ-metal shield. Before mounting the spectrometer the inner shield was demagnetized by a coil of twenty turns between the two shields. An ac current of 2.5 A through this coil was enough to demagnetize the inner shield, and to reduce the magnetic field to $\approx 10^{-8}$ T. The magnetic field cannot be measured after the spectrometer has been installed, however, it is expected to be less than 5×10^{-8} T.

The electric field between the two concentric cylinders is terminated at both ends by a set of thirteen concentric copper rings. They are dimensioned such that they divide the total potential difference between the cylinders in fourteen equal steps. The rings are positioned in two overlapping sets and form an optically closed shield.

The light source is a conventional differentially pumped gas discharge [12,13], suitable for the noble gases, and delivers predominantly the corresponding lowest resonance line. In the case of He it produces $\approx 2 \times 10^{10}$ photons/mm^2 s in the source volume of the spectrometer at a wavelength of 58.4 nm (21.22 eV).

The discharge is maintained in a quartz capillary of 28 mm length and 2 mm inner diameter. The pressure in the discharge capillary is ≈ 133 Pa. The lamp is operated at 80 mA and 300 V. After 3 or 4 weeks of continuous operation the capillary gets dirty and must be replaced.

The lamp and the spectrometer are separated by a capillary of 0.7 mm diameter and 10 mm length. There is no relevant increase of the background pressure in the spectrometer (1.3×10^{-5} Pa) when the pressure in the lamp is increased to 133 Pa. The vacuum ultraviolet (VUV) radiation from the lamp passes through the bottom part of the spectrometer inside a quartz capillary of 1 mm inner diameter; the length of this capillary is 120 mm. The inner surface of this capillary is covered with graphite to reduce reflections and the angular spread of the photon beam to a minimum in order to minimize the number of secondary electrons formed when photons strike a metal surface.

During the experiments the intensity of the photon beam is monitored by the current of secondary electrons from a simple copper surface at the opposite side of the spectrometer.

Gas is led into the source volume of the spectrometer by a conically shaped gas inlet. The tip of

this cone is positioned at the intersection of the light beam and the symmetry axes of the spectrometer. A mixture of gases may be supplied through the gas inlet. The pressure in the source volume is enhanced by a factor 40 relative to the background pressure. This enhancement factor is larger than the one that can be achieved by a single inlet channel at the same distance from the opening.

Mass selection is realized by a "time-of-flight" (TOF) spectrometer. Ions are extracted from the reaction volume by a triggered double pulse on the first two electrodes of an acceleration system. The reaction volume is defined as the cylindrical volume above the hole of the first electrode of the TOF spectrometer, and comprises the source volume of the electron spectrometer. Usually the potential of the first electrode is zero so that the reaction volume is field free. The second electrode is kept at 2 V positive to prevent ions to leak into the acceleration region. The holes of the first two electrodes have 6 mm diameter and are covered with a mesh. When ions are to be detected and mass analyzed, two negative pulses of 60 and 90 V (and 15 ns rise time) are applied to the first two electrodes. The ions are thus swept out of the reaction volume, accelerated further, and, after passing a field-free drift region, finally detected by two microchannel plates in tandem (25 mm diameter). The field-free drift region is dimensioned such that space focusing is achieved [14]. This means that the total flight time of the ions is, in first order, independent of the starting point in the reaction volume. There are two reasons for using channel plates instead of a channeltron. The large effective area of the channel plate reduces discrimination of ions with initial velocities perpendicular to the symmetry axes. The second advantage is that the flat surface of the channel plate allows an accurate definition of the flight time of the ions. The mass resolution achieved is $m/dm = 40$.

3. Electronics

In fig. 2 a schematic view of the electronics is given. The system is built around a Tracor TN-1700

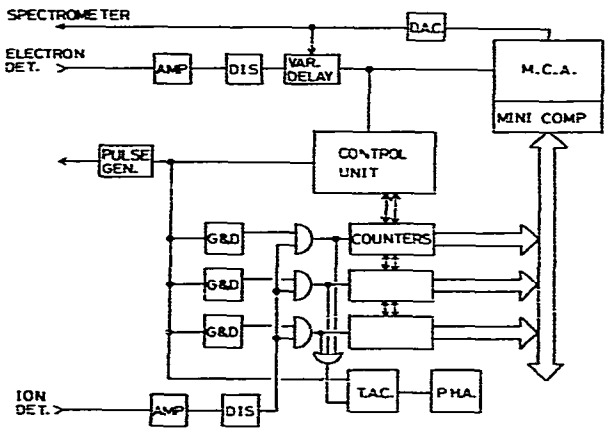

Fig. 2. The scheme of the coincidence electronics

multichannel analyser (MCA), based on a Nova computer. The singles electron spectrum is directly measured in the MCA, which scans the voltage of the electron spectrometer by means of a digital to analog converter. The electron signal triggers a control unit that determines whether a correlated or an uncorrelated TOF measurement will be performed. For the case of an uncorrelated measurement the electron signal is delayed for an extra 100 μs, enough to guarantee statistical conditions in the reaction volume. The control unit directs the counters and triggers the pulse generator, the gate and delay generators (G&D) and the TAC. The G&Ds are used to set time-windows in the time/mass spectrum. When an ion signal is coincident with one of these windows it is counted in the appropriate counter. At every step of the MCA the contents of the counters are read by the computer. The TAC and a second MCA, used in the pulse height analysis (PHA) mode, are used to monitor the performance of the TOF spectrometer and the positions of the time windows.

The electrons detected by the electron spectrometer are not accelerated to a fixed transmission energy. As a consequence their transit time is a function of energy. Since the ion extraction pulse is triggered by the electrons one has to account for these different transition times in order to guarantee a reaction time span for the coincident ions which is independent of electron energy. We have

achieved this correction by means of a variable delay unit, controlled by the voltage of the spectrometer. It contains an analog module to calculate the square root of the selected energy and a programmable delay. The variable transit time of the electrons is in this way corrected to a constant time of 0.7 μs, which corresponds to the transit time of 2 eV electrons. The accuracy of the correction is 15 ns.

The double-pulse generator, used for the ion extraction pulses on the first two electrodes of the TOF spectrometer, is a home-made device based on power-mosfets and capable of producing negative pulses of 100 V into two 50 Ω loads with a rise time of less than 15 ns. The second electrode has a dc offset relative to ground of 2 V to prevent ions from drifting into the acceleration region when no pulses are applied.

For the experiment a number of special counters are built and connected to the bus of the computer based multichannel analyser. These counters consist of binary up/down counters in combination with a buffer. The computer software is altered in such a way that every time the MCA increases its channel pointer the contents of the counters are dumped into the buffers, and the counters are cleared and restarted. Afterwards the contents of the buffers are read by the computer and added at the appropriate places in the memory. The great advantage of this procedure is that the counters function without deadtime. For most experiments six external counters are used, resulting together with the original MCA spectrum in seven simultaneously measured spectra. The counters can be operated in two modes; as up/down counters, or as gated counters. In both modes the steering signal can be the correlated/uncorrelated signal of the experiment or some external signal. The counters can be addressed by the computer as individual counters or as an array.

4. Method of measurement

To describe the method that allows us to measure the relative reaction probabilities for different internal energies of the molecular photoions, we consider, as an example, the system H_2^-/He. Both H_2 and He are present in the field-free ionization-reaction volume. H_2 is ionized by the UV photons of fixed energy ($h\nu = 21.22$ eV) and $H_2^-(v)$ is formed in various vibrational states with probabilities determined by the Franck–Condon factors.

$$h\nu + H_2 \rightarrow H_2^-(v) + e(\epsilon_v). \tag{4}$$

The photoelectron corresponding to formation of a H_2^- ion in a certain vibrational state (v) has a well defined energy ϵ_v determined by energy conservation.

Let us assume an electron of energy ϵ_i is detected. At the time of detection the corresponding ion $H_2^-(v)$ is still very close to the position where it was formed. On the average it takes a few microseconds until it leaves the reaction volume. After a delay of (in this case) 1 μs the TOF measurement is triggered, resulting in the extraction of all the ions in the reaction volume. During this time interval the primary ion has had the opportunity to collide with a He atom and to form a secondary ion:

$$H_2^-(v) + He \rightarrow HeH^+ + H. \tag{5}$$

The delay of 1 μs is chosen such that there is only a small chance for the ion to leave the reaction volume. By scanning the electron spectrometer at otherwise fixed conditions a correlated signal is measured for both the primary and the secondary ions, $P(v)$ and $S(v)$ respectively. These correlated signals are the sum of a true coincident and an uncorrelated signal.

The uncorrelated signal appears because there is at any instant a possibility for a random ion, of primary or secondary ion mass, to be present in the reaction volume. For the parent ion this probability is given by the average residence time in the volume times the rate of ionization processes. For the secondary ions the probability is lower by a factor, which might be called the average reaction probability. Therefore the uncorrelated signals are pure reflections of the "singles" electron spectrum and may be expressed as

$$P'(v) = GC_p F(v), \tag{6}$$

$$S'(v) = GC_s F(v). \tag{7}$$

With C_p and C_s the random possibilities to be present in the source volume for primary, and secondary ions, respectively, G a constant containing the ion detection efficiency, and $F(v)$ the Franck–Condon factor for production of a H_2^+ ion in the vibrational state v.

The true coincident signal for primary and secondary ions can be formulated as follows,

$$P_c(v) = GF(v)[1 - W(v)], \tag{8}$$

$$S_c(v) = GF(v)W(v), \tag{9}$$

where $W(v)$ is the relative, vibrational-energy-dependent cross section for the reaction. These true coincident signals are measured as the differences of the corresponding correlated and uncorrelated signals:

$$P_c(v) = P(v) - P'(v), \tag{10}$$

$$S_c(v) = S(v) - S'(v). \tag{11}$$

The relative, vibrational-energy dependent cross section can now be calculated as

$$W(v) = S_c(v)/[S_c(v) + P_c(v)]. \tag{12}$$

There are several possibilities to measure the uncorrelated signals, as long as the TOF spectrometer is triggered by a random signal. The uncorrelated signal could, for instance, be measured before or after the measurement of the correlated signal. We rejected this method since it is sensitive to long-term variations in photon intensity and gas pressure.

In our early experiments we measured the uncorrelated signal directly by applying, after each extraction pulse triggered by an electron, a second pulse delayed long enough to guarantee "statistical conditions" in the reaction volume. It turned out that the second pulse for measuring the uncorrelated signal was not exactly the same as the correlated pulse. The result was that the mass/time spectrum corresponding to the second pulse was ≈ 1 ns shifted relative to the spectrum for the first pulse. The cause of this phenomenon is expected to be the different history for the two pulses. The first pulse is random in time, but the second always has a predecessor at a fixed time. This small shift, in combination with the fact that we use time-windows to select the ion masses and that the difference between correlated and uncorrelated signals is only 20–30%, introduces a significant error in the calculated true coincidence signals. The influence of this systematic error can be seen in our early results [1] for the reaction of H_2^+ with He, where the cross section for energies below threshold was slightly larger than zero. We have eliminated this systematic error by using a part of our electron signal to trigger, after a proper extra delay, the TOF spectrometer for the measurement of the uncorrelated signal. We have the possibility to measure – dependent on the needed statistics in the background signal – on a 1 : 1 to a 1 : 7 basis for the background to signal ratio.

5. Measurements and results

We have performed measurements on reactions (1)–(3) given in section 1. The reaction of D_2^+ with He could not be measured because in a mixture of D_2 and He both D_3^+ and HeD^+ appear as product ions. Since they have the same mass the TOF measurement cannot distinguish between them.

In fig. 3 a typical example of a measured set of spectra for reaction (1) is given. The lower spectrum is the photoelectron spectrum of H_2, clearly showing the vibrational levels of the H_2^+ ion. The upper two are spectra of electrons in coincidence with the ion masses of H_2^+ and HeH^+. They are obtained by subtracting the correlated and uncorrelated spectra. It is immediately visible in the spectra that no HeH^+ ions are formed in coincidence with electrons that leave the H_2^+ ion in one of the three lowest vibrational states.

The results for reaction (1) are given in fig. 4. In this figure the energy scale is relative to the energy of the zero vibrational level of H_2^+. The cross section is given in arbitrary units. The error bars indicate statistical errors. The endothermicity of this reaction is 0.803 eV [4]. The vibrational energy in the $v = 3$ level is 0.768 eV [16]. The small, non-zero, cross section for this vibrational level can therefore be explained by a contribution of thermal translational and rotational energy of ≈ 40 meV.

It is very reassuring to observe that the cross

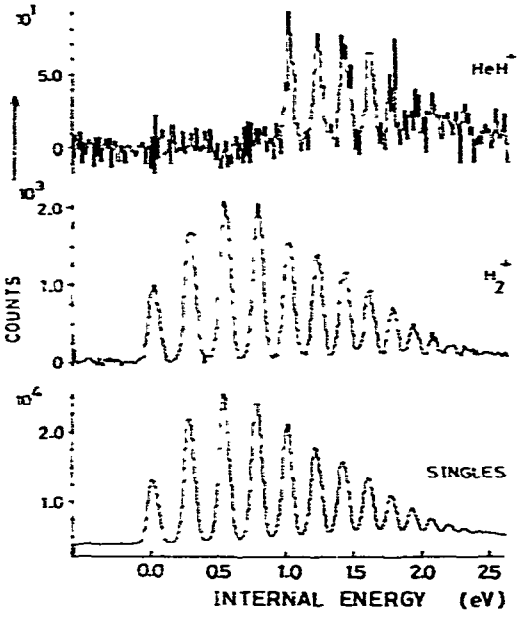

Fig. 3. Typical example of the measured spectra. The bottom spectrum represents the singles electron spectrum. The two upper spectra represent electrons coincident with H_2^+ and HeH^+. They are obtained by subtracting the corresponding correlated and uncorrelated spectra.

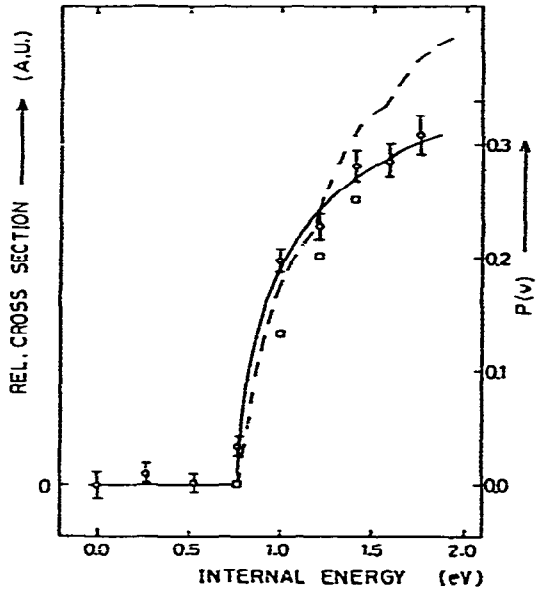

Fig. 4. The data for reaction (1): formation of HeH^+. The energy scale is relative to the zero vibrational level of H_2^+. The circles represent the present experimental results. The solid line, including the right-hand ordinate, is our fit as explained in section 6. The dotted line is a normalized prediction of phase space theory. The squares represent the calculations of Wagner et al. [17], given on the same scale as our fit.

section for the lowest vibrational levels is indeed zero within statistical errors. This supports the assumption that there are no relevant contributions to the measured cross sections from reactions during the process of acceleration in the TOF spectrometer, for those relative fast ions have enough translational energy to overcome the endothermicity.

The cross sections for reactions (2a) and (2b) are shown in fig. 5. The energy scale is relative to the energy of the zero vibrational level for both reactants. The endothermicity for the two reactions is 0.54 eV [4]. There is a small difference due to the different zero-point energies for the molecules with different isotopes. The nett effect on the endothermicity is, however, only 2 meV and cannot be observed in this experiment. The cross sections for both reactions seem to be rather insensitive to the internal energy when the energy is above 1 eV.

In fig. 6 the cross sections for reactions (3a) and (3b) are shown. Both cross sections are separately normalized. For both reactions the cross sections show a rather structureless decrease for increasing internal energy, without any discontinuous behaviour for a specific vibrational level. Moreover no significant differences can be noticed for H_2 and D_2.

Besides the reaction under study, charge transfer between a state-selected ion and a neutral hydrogen (deuterium) molecule is a possible process. In the case of vibrationally resonant charge transfer nothing changes on the state selection. Vibrationally non-resonant charge transfer, on the other hand, reduces the internal energy of the coincident ion and can therefore affect the measured energy dependence. In order to get some insight into the importance of non-resonant charge transfer in our experiments we performed two tests.

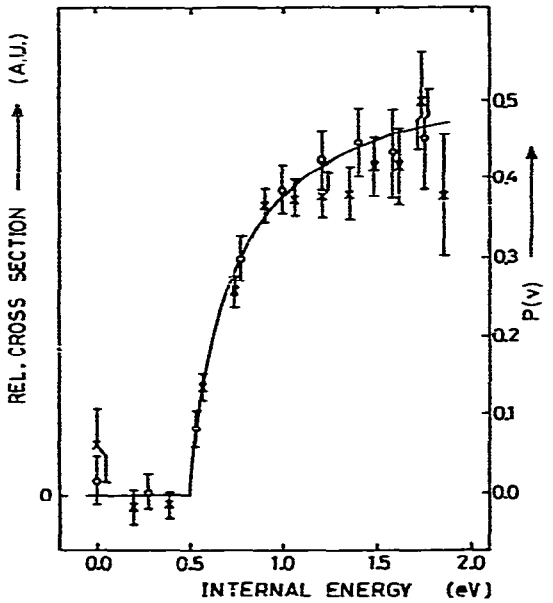

Fig. 5. The results for reaction (2a) (NeH^+: circles) and (2b) (NeD^+: crosses). The energy scale is relative to the zero vibrational level of both H_2^+ and D_2^+. The solid line, including the right-hand ordinate, is our fit as explained in section 6.

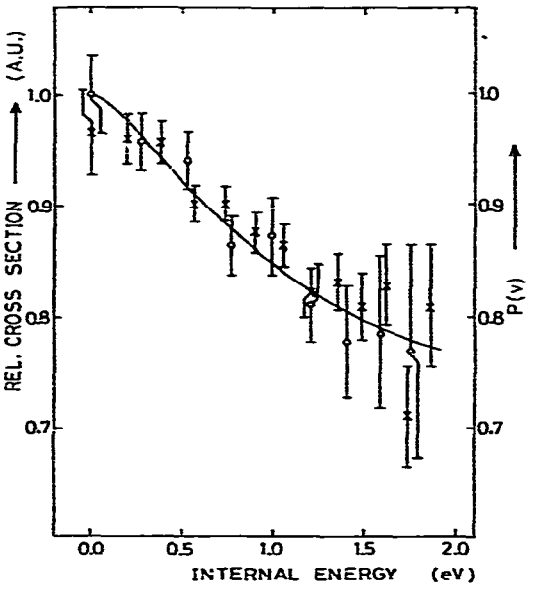

Fig. 6. The results for reaction (3a) (H_3^+: circles) and (3b) (D_3^+: crosses). The solid line, including the right-hand ordinate, is our fit as explained in section 6.

(i) Since the possible influence of non-resonant charge transfer is through a two-step process, it must be pressure dependent. Measurements at two different pressures, however, did not result in a difference in the energy dependence of the cross section.

(ii) We also performed measurements in a mixture of H_2 and D_2. If non-resonant charge transfer is important there should be some structure visible in the spectra coincident with H_2^+ that can be attributed to the D_2^+ electron spectrum and vice versa. The absence of this structure in the spectra enabled us to calculate an upper limit for the cross section of non-resonant charge transfer, relative to the cross section for particle transfer. We found that the cross section for charge transfer is smaller by at least a factor 4. This is consistent with the observation of Anderson et al. [7] who conclude that for translational energies below 1 eV rearrangement becomes the most important process. When their translational-energy-dependent reaction cross section is extrapolated to 40 meV a value of ≈ 70 Å^2 is found, whereas the cross section for charge transfer decreases strongly below 1 eV and reaches values significantly below 20 Å^2 if extrapolated to the thermal region.

Since in our experiments the probability for a rearrangement reaction is chosen to be $\approx 10\%$ the possibility for charge transfer is smaller than 2% and can therefore have no major influence on the measured energy dependence.

6. Discussion

Measurements on the internal energy dependence of reaction (1) have been reported by Chupka and Russell [4] for the vibrational levels $v = 0$–5. In their experiment, hydrogen, in a mixture with helium, was ionized by means of a wavelength-selected photon beam. The ions were formed between two repeller plates. The ion intensities for both hydrogen and hydride ions were measured as a function of the wavelength. The repeller voltage was kept zero during the experiments.

The photoionization efficiency curve of molecular hydrogen shows contributions due to two ionization processes. Strong autoionization lines

are superposed on a direct ionization continuum. It is assumed in ref. [4] that in the autoionization process the highest possible vibrational level is almost exclusively populated, in contrast to the direct process where a Franck–Condon distribution of vibrational states is produced. For a proper analysis of their experimental results, Chupka and Russell have to unravel those two contributions.

When we compare our results, for reaction (1), with those of ref. [4] we note, apart from a general agreement, a small difference for the cross section at $v = 3$. At this vibrational level the internal energy is less than the theoretically predicted value for the endothermicity of 0.803 eV. Chupka and Russell note that, as a consequence of 0.1 eV of translational and rotational energy the cross section at $v = 3$ is a third of the cross section at $v = 5$. Our results show a smaller value indicating that the kinetic energy in our experiment is substantially lower.

Calculations based on a statistical model reported by Wagner and Truhlar [17] show a vibrational enhancement in general agreement with our measured relative cross section, but, since values for only three vibrational levels above threshold are given a detailed comparison of the energy dependence is not possible.

To compare the measured energy dependence with predictions of the phase space theory, we performed computer calculations according to a model proposed by Chesnavitch and Bowers [18,19]. In these calculations a collision complex is assumed with a certain energy E and an angular momentum J. The possibility for dissociating in the forward direction is assumed to be determined by the number of available states in both forward and backward channel. The number of available states is calculated as follows. For a specific vibrational state, the energy available for translation and rotation is calculated from the total energy, the endothermicity and the vibrational energy. Then the number of rotational and translational states is calculated for which, given the available energy and the total angular momentum, the system is able to overcome the rotational barrier caused by the ion–induced dipole interaction. The calculated cross section for reaction (1) is compared with experiment in fig. 4. The calculated energy dependence cannot reproduce the experimental results.

Previous experimental data on reaction (2a) are reported by Chupka and Russell [4] for the vibrational levels $v = 0$ to $v = 4$, and are in agreement with our results. Previous results on reaction (2b) are not known to the authors. It is interesting to notice that the cross sections of reactions (2a) and (2b) behave equally and show no increase at the thresholds for vibrationally-excited products.

Reaction (3) has been the subject of many studies and much discussion has been devoted to the question whether or not this reaction behaves as a statistical one. By now there is a consensus that at least at kinetic energies above 1 eV a statistical approach is not in accordance with the experimental results. At lower kinetic energies, however, a statistical model cannot be excluded on experimental grounds; for instance the crossed-beam experiment of Hierl and Herman [20] becomes less explicit at these energies. Stine and Muckermann [21] calculated the potential energy surface for a planar H_3^- configuration and found that there is no well that might correlate to a more or less stable complex. These authors though explicitly concede the possibility for a dynamical complex where the system is trapped by rotational barriers. Such a phenomenon is most favored at low energies and large impact parameters.

Experimental results on the cross section of reaction (3) were reported by several authors. Chupka et al. [3] found in a non-coincident experiment a smooth decrease of 20% over an energy range of 1 eV ($v = 0$–5). The kinetic energy in their experiment was ≈ 1 eV. This is a somewhat stronger decrease than our results show: 23% over a 1.8 eV energy range. To compare these figures it must be noted that Chupka et al. define the cross section as the ratio H_3^+/H_2^+ whereas our definition is the ratio $H_3^+/(H_3^+ + H_2^+)$. Using our definition Chupka's result would be a 17% decrease. It is amazing to notice that Chupka, though working at a higher kinetic energy, found a stronger energy dependence. This in contrast with the general observation that the internal energy dependence becomes weaker when the kinetic energy is increased [5,7]. There are two possible reasons why the energy dependence reported by Chupka might be

somewhat too strong. In the first place, the separation in contributions due to direct ionization and autoionization is difficult to achieve accurately. A second source of a possible systematic error is that, since only the ion yield is measured, some forms of chemi-ionization could not be separated from reaction (3a). Since these processes contribute mostly near $v = 0$ the effect enhances the energy dependence.

More recently measurements on reaction (3) are reported by Koyano and Tanaka [5] and Anderson et al. [7]. Koyano and Tanaka used the TESICO (threshold-electron-secondary ion-coincidence) technique. They reported a decrease of the cross section of 14% for $v = 0$ to $v = 3$ at a collision energy of 0.1 eV, in accordance with our results. The results are compared in table 1. Anderson et al. used a guided-ion-beam technique and were able to separate reaction (3) into two contributions of proton and atom transfer. At a collision energy of 0.23 eV, they found a decrease of 14% over the range of $v = 0$ to $v = 4$ for proton transfer, but no energy dependence for atom transfer. Since both contributions are of the same magnitude, our result must be compared with the mean value of both proton and atom transfer. The resulting mean value of 7% is somewhat smaller than our value. This might be attributed to the difference in collision energy. We may, therefore, conclude that our results for reaction (3a) are in agreement with those of refs. [5,7].

Table 1
Cross sections of reaction (3)

v	Relative cross sections		
	this work	Koyano and Tanaka [5] [a]	Anderson et al. [7] [b]
0	1.00 ± 0.03	1.00 ± 0.05	1.00
1	0.96 ± 0.03	0.90 ± 0.05	0.94
2	0.94 ± 0.03	0.91 ± 0.07	0.93
3	0.86 ± 0.03	0.84 ± 0.06	0.92
4	0.87 ± 0.03		0.92
5	0.81 ± 0.03		
6	0.78 ± 0.05		
7	0.78 ± 0.07		
8	0.77 ± 0.09		
	Absolute cross sections (Å^2)		
	76	51	29

[a] Data retrieved from the figures in ref. [5], kinetic energy of 0.11 eV.

[b] Data retrieved from the figures in ref. [7], the kinetic energy was 0.23 eV in this experiment. As a reference we took the average of the proton and atom transfer cross section

Statistical theories for bimolecular reactions that go through a complex have been discussed extensively in the literature. A recent summary of the different versions is given by Light [2]. A detailed version designed for ion–molecule reactions is the one formulated by Chesnavitch and Bowers [18], which has been used by us to calculate the cross section dependence on reactant vibrational excitation for reaction (1). As is obvious from fig. 4, the disagreement with experimental data is drastic.

On the other hand, it should be stressed that the conditions under which reaction (1) is measured are very well suited for application of the statistical model, namely:

(i) The mutual relative kinetic energy in the reactant channel is small enough (≈ 40 meV) to guarantee that the Langevin radius R_L is large compared to the size of the $H_2^-(v)$-molecule [$R_L \approx 3.5$ Å for reaction (1)] so that the cross section of formation of the "close collision complex" is virtually independent of vibrational excitation of $H_2^-(v)$, as is assumed in the models.

(ii) The internal energy of the complex – carried into the complex in the form of vibrational energy of $H_2^-(v)$ – is large compared to the initial relative kinetic energy, in the range of internal energies subtended in our measurements. Therefore the phase space available for the system is large compared to the phase space belonging to formation of the complex, rendering a statistical decay, in which the initial conditions of formation are "forgotten", rather probable.

Because of these favourable conditions for statistical behaviour of reaction (1), and of the other reactions studied here, we believe that the failure to reproduce the experimental data by the statistical model is not caused by its principal inadequacy but rather by details of counting the available states in the dissociation channels.

This is also supported by the fact that, if in the case of reaction (1) the vibrational states are neglected in counting the possible states in the for-

ward and backward dissociation channel of the complex, a much better agreement with the experimental data is obtained.

We therefore try to evaluate our data in terms of a statistical model in which there is some built-in flexibility regarding the counting of available active states. Using this flexibility to get agreement with the experimental data will then yield information on the system. In any statistical model of a bimolecular reaction, that goes through a complex the reaction cross section is given by

$$\sigma_f = P_f(E)\sigma_c, \tag{13}$$

with σ_c the cross section for formation of the complex, and $P_f(E)$ the probability at given total energy E, of the complex to decay in forward direction. If only one final channel is assumed, $P_f(E)$ has the form

$$P_f(E) = N_f(E)/[N_f(E) + N_i(E)], \tag{14}$$

with $N_{i,f}(E)$ the number of states available at energy E in the initial and final channel. Such states are only available if $E_{i,f} = E - V_{i,f} > 0$ with $V_{i,f}$ the electronic energy of the separated particles in the initial and final channel, respectively, and $E_{i,f}$ the respective energies available for the various degrees of freedom of motion. The numbers $N_{i,f}$ are proportional to the corresponding densities of states $\rho_{i,f}(E_{i,f})$. Estimates on the densities for the case of no constraints have been obtained on the basis of the "rigid-rotor-harmonic-oscillator" (RRHO) model for the cases of channels containing an atom and a diatomic molecule, or two diatomic molecules, as given by Levine and Kinsey [22]. These densities have the following general form

$$\rho(E_R) = A_R(E_R)^{n+3/2}, \tag{15}$$

with $n = 1$, 3 for atom–diatom, and diatom–diatom channels, respectively, and A_R structural factors that contain the reduced masses, rotational constants, and vibrational frequencies. The general form of the density functions given by eq. (15) suggests to use the same form but with an adaptable power s in order to build in the necessary flexibility. A power $s < n + 3/2$ determined by a fit to experimental data – if a fit is possible – then would indicate some constraints on the actual motion. Using such density functions $A_R(E_R)^{s_R}$ for forward and backward channel one obtains from (14)

$$P_f(E) = [1 + C_{if}(E_i^{s_i}/E_f^{s_f})]^{-1}, \tag{16}$$

with $C_{if} = A_i/A_f$, the ratio of the structural factors. Application of expression (16) to our experimental data is especially simple because our relative cross sections $\sigma(v)$ are obtained under the same initial collision conditions – i.e. with the same value of σ_c – so that $\sigma(v) \propto P_f(E(v))$. The total energy of the system, relative to the ground state of the initial channel, is $E = E_{vib} + E_{th}$, with E_{vib} the vibrational energy of $H_3^+(v)$, and E_{th} the thermal energy carried into the system. Since E_{th} is small compared to the vibrational quanta of $H_3^+(v)$, it is sufficient to characterize a complex by E_{vib} and by the average thermal energy $\overline{E_{th}}$. With Q, the exothermicity of the reaction, we then obtain from (16) the following expression for our relative cross sections

$$\sigma(v) = C\left[1 + C_{if}\left(E_{vib} + \overline{E_{th}}\right)^{s_i} \times \left(E_{vib} + \overline{E_{th}} + Q\right)^{-s_f}\right]^{-1}, \tag{17}$$

where C is a constant.

The parameters s_i and s_f cannot be fitted independently, but they must have a fixed difference $\Delta s = s_f - s_i$. The value C_{if} must be in accordance with this difference. Apart from the overall constant there is therefore only one parameter that can be fitted by comparison with the experimental data. For reactions (1) and (2) the difference Δs is

Table 2
Numerical values relevant to the fit. In accordance with the definition of the structural factor C_{if}, this quantity has a dimension (energy)$^{\Delta s}$ in cases where $s_i \neq s_f$. The index zero indicates the unmodified RRHO values (see text)

	C_{if}	Q (meV)	s_0		s	
HeH^+	1.62	−803	5/2		0.61 ± 0.09	
NeH^+	0.83	−545	5/2		0.83 ± 0.10	
	C_{if}	Q (meV)	s_{i_0}	s_{f_0}	s_i	s_f
H_3^+	90 (meV)$^{1/2}$	1700	9/2	10/2	1.86	2.36 ± 0.30

kept zero since both channels have the same atom–diatom configuration. For reaction (3), on the other hand, the difference was kept 1/2, reflecting the difference in the energy dependence of the state densities for a diatom–diatom, and a triatom–atom system. The state density for the triatom–atom system is calculated assuming that H_3^- is a spherical top. In figs. 4 and 5 the experimental data are compared with the ones calculated from (17) with a power s obtained from a least-squares fit. In table 2 the powers s are given and compared to the powers s_0 predicted for the case of no constraint, also given are the constants C_{if} used in (17). In the values for C_{if} an additional factor 0.5 is included to account for the deviating rotational density of the homonuclear diatomic molecules [17]. When in the fit procedure the parameters s_i and s_f have a fixed non-zero difference Δs, as in the case of reaction (3), the numerical value of the constant C_{if} is a function of s_i. This variation of C_{if} is taken into account by interpolation between the known values of C_{if} for half integer values of s_i (and s_f).

It should be pointed out that part of the differences $(s_0 - s)$ is due to the constraint of total angular momentum conservation. Further, if no vibrational excitation of the diatomic molecule occurs in the decay of a triatomic complex, s_0 is reduced by one unit giving $s_0 = 3/2$. Close to the reaction threshold therefore, s should not exceed this value. The numbers found for s may therefore be considered as physically reasonable within the model. The fact that all three reactions – two endothermic ones and one exothermic – are well described by our formula (17) we take as a strong indication that these thermal energy reactions go through a "complex" whose decay is well described by statistics with certain constraints.

Fitting our data with (17) leads to an accurate determination of the difference of the endothermicity for reactions (1) and (2): This difference is 258 ± 16 meV. When we use the value of 803 meV [4] for the endothermicity of reaction (1) we find a value of 545 ± 16 meV for the endothermicity of reaction (2). Since the difference in endothermicity is only due to the different dissociation energies for HeH^+ and NeH^+, we can calculate the dissociation energy of NeH^+ by using the theoretical value of 1.8441 eV for the dissociation energy of HeH^+ [23]. This leads to the value of 2.102 ± 0.016 eV for the dissociation energy of NeH^+, in good agreement with both theoretical and experimental values [23].

It should be stressed that by fitting our data with eq. (17) we determine the fraction of close collision complexes that dissociate into the product channel. This fraction $P(v)$ is given by the right-hand ordinate in figs. 4–6. The absolute cross section for the formation of these complexes can easily be calculated [15]: $\sigma_c(H_2^+/He) = 38$ Å^2, $\sigma_c(H_2^+/Ne) = \sigma_c(D_2^+/Ne) = 54$ Å^2 and $\sigma_c(H_2^+/H_2) = \sigma_c(D_2^+/D_2) = 76$ Å^2. By multiplying these absolute cross sections by the reaction possibility $P(v)$ obtained from the fit, the absolute cross sections can be calculated.

Absolute cross sections for reaction (1) are calculated by Wagner and Truhlar [17]. These calculations are represented by the squares in fig. 4, where they are given on the same scale as the fit through our experimental results. From this figure we can conclude that the absolute scale that we found for reaction (1), by fitting the results with eq. (17), is in agreement with the calculated absolute cross sections of ref. [17].

For reaction (3) we can compare our absolute values with those of Koyano and Tanaka [5] and Anderson et al. [7]. The absolute scale for the relative cross sections is also given in table 1. The fact that our value is larger than those of refs. [5,7] can be ascribed to the different kinetic energies. When we scale the value of Koyano and Tanaka according the $1/E^{1/2}$ energy dependence of the Langevin cross section from 110 to 40 meV, a value of 84 Å^2 is obtained. The same scaling procedure applied to the results of Anderson gives a value of 69 Å^2. We can therefore conclude that our absolute cross section for reaction (3) is in agreement with those of refs. [5,7].

Acknowledgement

This work was performed as part of the research programme of the Stichting voor Fundamenteel Onderzoek der Materie (FOM) with financial support from the Nederlandse Organisa-

tie voor Zuiver-Wetenschappelijk Onderzoek (ZWO).

References

[1] D. van Pijkeren, J. van Eck and A. Niehaus, Chem. Phys. Letters 96 (1983) 20.
[2] J.C. Light, in: Atom–molecule collision theory, ed. R.B. Bernstein (Plenum Press, New York, 1979).
[3] W.A. Chupka, M.E. Russell and K. Refaey, J. Chem. Phys. 48 (1968) 1518.
[4] W.A. Chupka and M.E. Russell, J. Chem. Phys. 49 (1968) 5426.
[5] I. Koyano and K. Tanaka, J. Chem. Phys. 72 (1980) 4858.
[6] K. Tanaka, T. Kato and I. Koyano, J. Chem. Phys. 75 (1981) 4941.
[7] S.L. Anderson, F.A. Houle, D. Gerlich and Y.T. Lee, J Chem. Phys. 75 (1981) 2153.
[8] S.L. Anderson, T. Turner, B.H. Mahan and Y.T. Lee, J. Chem. Phys. 77 (1982) 1842.
[9] J.E. Draper and C. Lee, Rev. Sci. Instrum. 48 (1977) 852.
[10] H.E. Bishop, J.P. Coad and J.C. Riviere, J. Electron Spectry. 1 (1972/73) 389
[11] G.M. Renfro and H.J. Fishbeck, Rev. Sci. Instrum. 46 (1975) 620.
[12] H. Haberland, University of Freiburg, private communication.
[13] G. Schönhense and U. Heinzmann, J. Phys. E16 (1983) 74.
[14] W.C. Wiley and T.H. McLaren, Rev. Sci. Instrum. 26 (1955) 1150.
[15] G. Gioumousis and D.P. Stevenson, J. Chem. Phys. 29 (1958) 294.
[16] J.E. Pollard, D.J. Trevor, J.E. Reutt, Y.T. Lee and D.A. Shirley, J. Chem. Phys. 77 (1982) 34.
[17] A.F. Wagner and D.G. Truhlar, J. Chem. Phys. 57 (1972) 4063.
[18] W.J. Chesnavich and M.T. Bowers, J. Chem. Phys. 68 (1978) 901.
[19] W.J. Chesnavich and M.T. Bowers, J. Chem. Phys 66 (1977) 2306.
[20] P.M. Hierl and Z. Herman, Chem. Phys. 50 (1980) 249.
[21] J.R. Stine and J T. Muckermann, J. Chem. Phys. 68 (1978) 185.
[22] R.D. Levine and J.L. Kinsey, in: Atom–molecule collision theory, ed. R.B. Bernstein (Plenum Press, New York, 1979).
[23] P. Rosmus and E.A. Reinsch, Z. Naturforsch. 35a (1980) 1056